Textural and Chemical Properties of Activated Carbon Prepared from Tropical Peat Soil by Chemical Activation Method

Tumirah Khadiran,[a,b] Mohd Zobir Hussein,[a,]* Zulkarnain Zainal,[a] and Rafeadah Rusli [b]

Activated carbon (AC) was produced *via* phosphoric acid (H_3PO_4) and zinc chloride ($ZnCl_2$) chemical activation methods at 500 °C for 3 h. Tropical peat soil was used as a carbon precursor. The effects of activating agent concentrations on the microstructure and chemical properties of activated carbon were studied. Activated carbon with a high BET (Brunauer-Emmett-Teller) specific surface area (S_{BET}) and a high total pore volume (V_{pore}) was produced using a 30% H_3PO_4 chemical activation method. The S_{BET} and V_{pore} of the activated carbon at this condition were 1974 m^2/g and 1.41 cm^3/g, respectively. However, the activated carbon prepared using $ZnCl_2$ activation only had a S_{BET} of 794 m^2/g and a V_{pore} of 0.11 cm^3/g. The nitrogen adsorption-desorption isotherms of both activated carbons exhibited a combination of Type I and Type II isotherms, due to the simultaneous presence of micro- and mesopores structures. The microcrystallinity of the activated carbons was characterized using an X-ray diffractometer and a Raman Spectroscopy, respectively. The activated carbon produced using H_3PO_4 activation had higher crystalline properties than the activated carbon prepared using $ZnCl_2$ activation. Thus, this article demonstrates the potential of tropical peat soil as a precursor of AC production.

Keywords: Chemical activation method; Phosphoric acid; Zinc chloride; Tropical peat soil; Activated carbon; Surface chemistry; Thermal energy storage

Contact information: a: Material Synthesis and Characterization Laboratory (MSCL), Institute of Advanced Technology (ITMA), Universiti Putra Malaysia, 43400 Serdang, Selangor, Malaysia; b: Forest Product Division, Forest Research Institute Malaysia (FRIM), 52100 Kepong, Selangor, Malaysia;
** Corresponding author: mzobir@upm.edu.my*

INTRODUCTION

Activated carbons (AC) are highly versatile inorganic materials that are commonly used as adsorbents. The demand for AC has increased over the years for a wide range of industries, such as the electrochemical industry (Frackowiak and Béguin 2001; Selvakumar and Bhat 2012) for electrode materials preparation, purification systems for wastewater, air, and water sources (Petrova *et al*. 2010), adsorbents of heavy metals (Mochida *et al.* 2012; Olorundare *et al*. 2012), support for catalyst reactions (Skubiszewska-Zieba 2010), batteries (Fernández *et al*. 2010), and others. This encourages many studies on the search and development of eco-friendly and low-cost AC.

Recently, researchers have started to use AC as an inorganic framework for the preparation of thermal energy storage (TES) based on phase change material (PCM) (Feng *et al*. 2011; Wang *et al*. 2012; Chen *et al*. 2012). AC is highly attractive as an inorganic framework for the preparation of TES material due to its low density, good thermal conductivity, chemical stability, well-defined pore structure, high specific surface area, and relatively low cost. The findings from Chen *et al*. (2012) indicated that AC can improve the thermal stability of the PCM composites as the carbonaceous layers create a physical protection barrier on the surface of the composite. This was due to the porous carbon materials of AC that effectively stabilized the PCM through both the capillary forces of the pores and the hydrogen bonding created by the functional groups of AC (Wang *et al*. 2012). However, Wang *et al*. (2012) reported that the performance of composite AC/PCM depends on the pore structure of the AC. Therefore, the researchers suggested that proper control of the pore structure of the supporting materials is critical to improving the performance of the resulting composite PCM. Hence, the pores of AC should be properly engineered to fulfill the requirement as an inorganic framework in TES technology. TES based on PCM is widely used in various industries, such as in buildings, transportation, textiles, electronics, and others.

In general, the specific characteristics of AC, such as BET specific surface area, pore structure, and chemical polarity depend on several factors, especially the type of carbon precursor and activation method (González-Garía *et al*. 2013). Other parameters, such as carbonization temperature, carbonization time, impregnation ratio, and the activating agent used during the carbonization and activation processes, are also important. The industrial application of solid adsorbents with a relatively large pore size distribution can be obtained through a chemical activation process (Torregrosa-Macia *et al*. 1997). It was also reported that chemical activation is one of the common processes used in the commercial preparation of AC (Yang and Lua 2006). The chemical activation method could be used to develop the desired pore structure (Caturla *et al*. 1991; Bahri *et al*. 2012).

Chemical activation consists of impregnation of the precursor with chemicals that can act as catalysts, such as phosphoric acid (H_3PO_4) (Fierro *et al.* 2010; Tham *et al*. 2011; Olorundare *et al*. 2012), alkali metal hydroxide (KOH, NaOH) (Otawa *et al*. 1997; González-Garía *et al*. 2013), zinc chloride ($ZnCl_2$) (Ibarra *et al*. 1991; Nohara *et al*. 2005), potassium carbonate (K_2CO_3) (Liu *et al*. 2012), and many others. However, among the activating agents available, H_3PO_4 is more preferred due to its environmental soundness (lower environmental and toxicological problem) (Bahri *et al*. 2012), while $ZnCl_2$ is chosen due to its effective activating capabilities (Torregrosa-Macia *et al*. 1997; Caturla *et al*. 1991; Yang and Lua 2006). The correct selection of the activation agent could produce a good textural and chemical property of AC, making AC potential candidates for various applications.

AC can be produced from a variety of carbonaceous materials that are carbon rich and have low ash contents, such as agricultural waste, industrial waste, coal, *etc*. The agricultural wastes are more suitable as a feedstock since they are renewable sources having low cost (Stavropoulo *et al*. 2005). Many agricultural wastes, such as coconut shells (Mozammel *et al*. 2002; Sekar *et al*. 2004), rubberwood sawdust (Srinivasakannan and Bakar 2004), fruit stone (Puziy *et al*. 2005), durian shell (Tham *et al*. 2011), bamboo (González-Garía *et al*. 2013), and others, have been discovered to be suitable precursors for AC preparation. Industrial wastes such as waste tire (Ariyadejwanich *et al*. 2003), waste sludge (Khalili *et al*. 2000), and leather waste (Kong *et al*. 2013) were also reported to be successful precursors for the AC production.

Peat soil is also one of the carbon rich materials. Peat soil consists of partly decomposed leaves, branches, twigs, and tree trunks with low mineral content, but rich with celluloses, hemicelluloses, and lignin. Therefore, it is also considered a suitable precursor for the production of AC. Peat soils occupy a total area of 2.7 million hectares (Mha) in Malaysia, accounting for about 8% of the country's total land area (Mutalib *et al*.

1992). Unfortunately, peat soil has been regarded as a problematic soil due to its high acidity and low levels of available nutrients (Wong 1991; Cheong and Ng 1977); thus, it is not suitable for the crop industry. In addition, peat soil has very low bearing capacity and shear strength (Islam and Hashim 2010), and thus, it is not suitable for the construction of buildings, highways, or any other load-bearing engineering structures. The conversion of peat soil into AC would increase the economic value of peat soil and provide a potentially inexpensive raw material for local commercial AC production.

In this study, the activation of peat soil was carried out using the chemical activation method. H_3PO_4 and $ZnCl_2$ were used as the activating agents. The emphasis of this study was to optimize the process to tailor the AC with excellent pore structure parameters (BET specific surface area, pore volume, and average pore diameter) and surface chemistry. In order to minimize the loss of energy storage capacity in TES materials, the inorganic frameworks-based AC need to have suitable pore structure and surface chemistry characteristics. It is expected that the large surface area and low density of an inorganic framework AC will enhance the shape stabilized capabilities and thus minimize the loss of energy storage capacity of PCM (Wang *et al*. 2012).

To our knowledge, there have been only two publications about the use of tropical peat soil as a precursor for AC production (Uraki *et al*. 2009; Ogawa *et al*. 2011). They used a physical activation method and emphasized on the application of the product for water treatment. To the best of our knowledge, the use of the peat soil as a carbon precursor, activated using the chemical activation method, has not been previously described in the literature. There has been no report on the utilization of AC derived from peat soil, using physical or chemical activation methods, as an inorganic framework in the field of TES-based PCM. Therefore, we took this opportunity to investigate the properties of AC prepared from peat soil by several activation agents. The study suggested that the pore structure parameter of AC derived from peat soil could be tailored by controlling the activating agent concentration and the type of activation agent. The findings from this study suggested that the obtained AC has potential to be used in various applications, including as an inorganic framework for the preparation of shape-stabilized phase change materials, which finally could be applied in TES.

EXPERIMENTAL

Materials

Peat soil was collected in the Sabak Bernam area of Malaysia. It was then oven-dried at 60 ^oC for 48 h, ground, sieved through a 0.5 mm sieve, and kept in a desiccator as a raw material for AC production. The characterization of the peat soil is shown in Table 1. Analytical reagents grade chemicals purchased from Sigma-Aldrich were used in this study.

The fiber content of the peat soil sample was determined based on the dry weight of fibers retained on ASTM sieve no. 100 over the total oven dried mass sample as according to ASTM D 1997-91 method. The moisture content of peat soil samples was determined by drying the peat soil sample in an oven at 105 ^oC for 24 h according to ASTM D 4318. The elemental content (carbon, hydrogen, nitrogen, oxygen, and sulfur) of peat soil samples was determined using CHNSO analyses. The hemicellulose, cellulose, and lignin content were determined based on procedures stated by Wise *et al*. (1946), TAPPI

T203 om-93 and TAPPI T222 om-02, respectively. The pH test of peat soil sample was conducted according to the procedure mentioned in BS 1377-1990.

Table 1. Proximate, Ultimate, and Main Components of Peat Soils (% dry basis)

Moisture content of peat soil	345
Fiber content	79.5
Ash content	9.1
C	52.8
H	4.6
N	1.3
S	0.1
O	0.1
Hemicellulose	2.1
Cellulose	10.6
Lignin and lignin-derived substances	75.0
pH	3.5

Preparation of Peat Soil Activated Carbon

H_3PO_4 and $ZnCl_2$ were used as the activation agents. In the case of H_3PO_4, 5 g peat soil was impregnated with a 50 mL solution of 1, 5, 10, 20, and 30% H_3PO_4 and left at 70 ^oC in an oil bath shaker (100 rpm) for 24 h or until all the excess water was evaporated. The time required to evaporate the excess water in the impregnated samples varied depending on the amount of H_3PO_4 used for the activation processes. A higher activating agent concentration required a longer drying time. The samples were then oven-dried at 120 ^oC overnight. After they were oven-dried, the sample in the sludge form was crushed again into fine powder, transferred into a crucible, and carbonized at 500 ^oC for 3 h in a tubular electric furnace under an inert flow of nitrogen (N_2) gas with a flow rate of 100 cm^3min^{-1}. The heating rate of 10 ^oC min^{-1} was used in this study. The resulting AC was cooled to room temperature and refluxed with water for 24 hours, followed by being washed with distilled water. The AC samples were then oven-dried overnight. The dried AC samples were transferred into a sample bottle and kept in a desiccator for further characterization.

Table 2. AC Prepared using H_3PO_4 and $ZnCl_2$ Activation Agent at 500 ^oC for 3 h

Label	Chemical method	Conc. (%)	Label	Chemical method	Conc. (%)
PSAC-P-1	H_3PO_4	1	PSAC-Z-1	$ZnCl_2$	1
PSAC-P-5	H_3PO_4	5	PSAC-Z-5	$ZnCl_2$	5
PSAC-P-10	H_3PO_4	10	PSAC-Z-10	$ZnCl_2$	10
PSAC-P-20	H_3PO_4	20	PSAC-Z-20	$ZnCl_2$	20
PSAC-P-30	H_3PO_4	30	PSAC-Z-30	$ZnCl_2$	30

PSAC-P: Peat soil activated carbon prepared using the H_3PO_4 activation method
PSAC-Z: Peat soil activated carbon prepared using the $ZnCl_2$ activation method

A similar technique was used for preparation of AC using the $ZnCl_2$ chemical activation method. For this technique, however, the resulting AC were refluxed with 0.2 M nitric acid (HNO_3) for 6 h and then washed with distilled water three times to remove excess $ZnCl_2$ from the AC samples. The label for the AC prepared in this study is summarized in Table 2.

Characterization of Peat Soil Activated Carbon

The physical characteristics of the peat soil and the resulting peat soil activated carbon (PSAC) samples were analyzed using N_2 adsorption-desorption, X-ray diffraction (XRD), and a Raman spectrometer. The textural characteristics of peat soil and PSAC samples were determined by N_2 adsorption-desorption at 77 K with a Quantachrome Instruments version 2.01, and the data were analyzed using its software package. The AC samples were first degassed at 290 ^{o}C under a vacuum for at least 24 h before the measurements. The BET specific surface area, pore volume, and average pore diameter of the PSAC samples were determined using the Brunauer-Emmet-Teller (BET) equation. The pore size distribution was calculated using desorption Barret-Joyner-Halenda (BJH) equation. The powder X-ray diffraction pattern of peat soil and PSAC was obtained using a Shimadzu XRD-6000 powder X-ray diffractometer (PXRD) at room temperature. A scanning range of 10 to 35^{o} (2θ) with a scanning rate of 4^{o} min^{-1} was employed. Raman spectra of the peat soil and PSAC were measured using a Ranishaw Raman spectrometer, cooled under liquid nitrogen. Raman wavenumbers were obtained using a laser excitation wavelength at 514.5 nm. The intensity ratio between the D-line (1350 cm^{-1}) and the G-line (1580 cm^{-1}) of Raman spectra was used to evaluate the graphitic character of the samples. The surface chemistry characterization of the peat soil and PSAC was performed by Fourier transform infrared spectroscopy (FTIR). The technique was used to identify its surface functional groups. The chemical characterization of the functional groups of peat soil and PSAC was analyzed by a Perkin Elmer BX spectrophotometer. The samples were mixed with KBr; then the absorbance spectrums were recorded in the range, 280 to 4000 cm^{-1}. The analysis was carried out at room temperature. The surface morphology and microstructure of the peat soil and PSAC were observed using a NOVA NANOSEM 230 field emission scanning electron microscope. The dried samples were dispersed on a conductive carbon adhesive tape surface attached to a FESEM stub and were then Au-Pd coated. Thermogravimetric experiments were carried out using thermal gravimetric analysis (TGA) (Q500 V20.13 Build 39, TA Instruments) at a heating rate of 5 ^{o}C min^{-1} under a N_2 atmosphere to investigate the activation and carbonization processes. Approximately 10 mg of the peat soil samples, impregnated peat soil-H_3PO_4 and impregnated peat soil-$ZnCl_2$, were heated from room temperature to 1000 ^{o}C. Derivative thermal gravimetry (DTG) was also used to determine the maximum rate of weight loss of the organic compound. The preparation of PSAC was repeated for two times (Table 2).

RESULTS AND DISCUSSION

Physico-chemical Properties of Peat Soil

Table 1 shows the physico-chemical properties of the peat soil samples used in this study. The moisture content of the peat soil is quite high, which is 343%. A similar finding was also reported by previous authors (Lucas 1982; Wust *et al*. 2003). In some cases, the moisture content of the samples is slightly low due to loss of pore water during transportation or storage (Wust *et al*. 2003). The organic constituents (hemicellulose, cellulose, and lignin) tested for the peat soil samples accounted for more than 80%. The fiber content was also high, at around 79%. The content of fiber and organic constituents are directly proportional to the specific gravity of the sample. An increase in the fiber and organic constituents can be expected to result in the decreasing of the specific gravity (Den Haan 1997). The results also show that peat soil had a pH value of 3.5 which is acidic. The concentration of carbon and hydrogen in the sample shows that the peat soil has the characteristic composition of the biomass materials (Ioannidou and Zabaniotou 2007).

Thermal Analysis

Figure 1 (a-b) shows the TGA and DTG thermograms of the peat soil sample, as well as peat soil impregnated with 30% H_3PO_4 (PS-PI) and $ZnCl_2$ (PS-ZI). The emphasis of this study was to investigate the activation and carbonization mechanisms in terms of the effect of the activating agent against the activation temperature. The TGA/DTG analyses was also used in order to predict their respective contributions to the chars and the subsequent activated carbons in term of weight fraction and contribution to the different porous properties such as microporosity, mesoporosity, and macroporosity (Cagnon *et al*. 2009). A weight loss of approximately 57.49 wt.% in the range of 25 ^oC to 860 ^oC was observed in the peat soil samples due to evaporation of water content (below 120 ^oC), decomposition of hemicellulose, cellulose, and lignin (200 ^oC to 520 ^oC), and resultant char (520 ^oC to 860 ^oC). The residue of 42.30 wt.% (860 ^oC to 100 ^oC) was assigned to the carbon constituent. As can be observed in the TGA thermogram of peat soil samples, the study suggested that at 800 ^oC to 1000 ^oC, the low boiling point and low melting point of organic matter in the peat soil samples were totally evaporated, while carbon remained. Similar findings were observed from other carbonaceous materials such as *Jatropha curcas* fruit shells (Tongpoothorn *et al*. 2011).

As compared with the TGA thermogram of peat soil, the TGA thermogram of peat soil impregnated with 30% H_3PO_4 (PS-PI) presented a high weight loss at 133 ^oC to 500 ^oC, corresponding to the decomposition of hemicellulose, cellulose, and lignin, followed by weight loss at 198 ^oC to 430 ^oC for the peat soil impregnated with 30% $ZnCl_2$ (PS-ZI). It is noticeable that the weight loss of peat soil was higher than that of PS-PI and PS-ZI in < 500 ^oC. This was due to the H_3PO_4 and $ZnCl_2$ retarding the formation of tars, slowing down the degradation of peat soil during the carbonization processes.

The observation in Fig. 1 (a-b) shows that H_3PO_4 and $ZnCl_2$ helped in decreasing the pyrolysis temperature of peat soil. However, $ZnCl_2$ showed that it was not really suitable to be used as an activating agent for activating peat soil, due to the less oxygen content in the peat soil. Peat soil consists of partially decayed plant matter with low levels of oxygen content, which are responsible for the low reactivity between $ZnCl_2$ and the OH groups (Delgado and Mendez 2011) that are mainly found in the biopolymer sample. Therefore, the ability of $ZnCl_2$ to transform the biopolymer in the peat soil into the carbon structure was also lacking. In addition, peat soil has a complex chemical composition, which may retard the $ZnCl_2$ from catalyzing the degradation during impregnation processes.

As compared with $ZnCl_2$, H_3PO_4 was observed to be more suitable as an activating agent for peat soil. This may be related to the activation mechanism of H_3PO_4, which is believed to function as a dehydrating catalyst (Jagtoyen and Derbyshire 1993) by acid hydrolysis mechanisms (Molino-Sabio *et al*. 1995) that can promote decomposition of the precursor-based biopolymers with high volatile content, such as peat soil.

Based on the degradation temperatures of biopolymer materials in PS-PI and PS-ZI samples and previous findings (Hussein *et al*. 1996; Ahmadpour and Do 1997; Tham *et al*. 2011), 500 °C was chosen as the optimum carbonization temperature for this study to obtain the maximum AC yield with the desired properties.

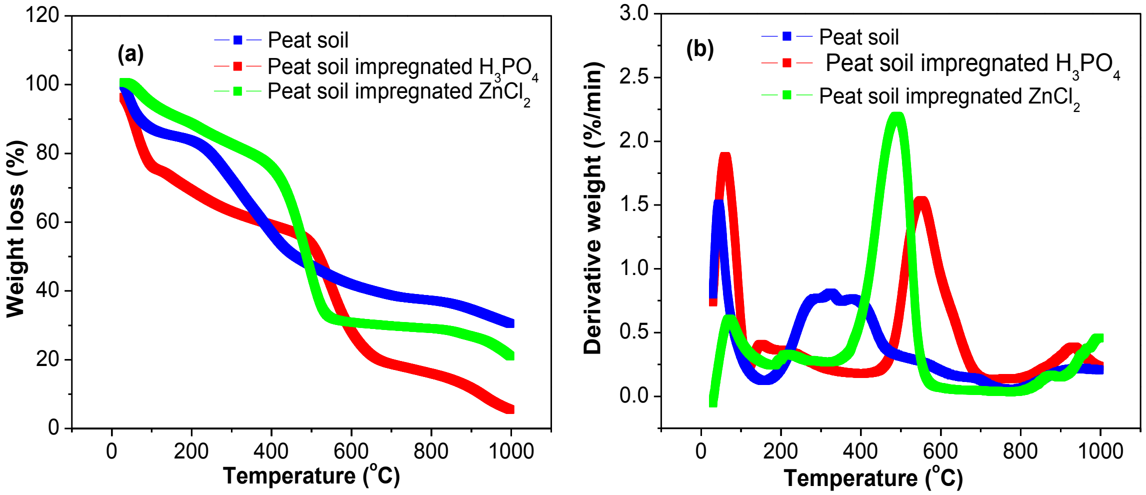

Fig. 1. (a) TGA thermograms of peat soil sample, peat soil impregnated with 30% H_3PO_4 (PS-PI) and peat soil impregnated with 30% $ZnCl_2$ (PS-ZI); and **(b)** DTG thermograms of peat soil sample, peat soil impregnated with 30% H_3PO_4 (PS-PI) and peat soil impregnated with 30% $ZnCl_2$ (PS-ZI)

Surface Morphology

The surface morphology of the peat soil, the peat soil sample impregnated with 30% H_3PO_4 and $ZnCl_2$ and carbonized at 500 °C for 3 h, labeled as PS-PIC and PS-ZIC, respectively, and the resulting PSAC-P-30 and PSAC-Z-30 were studied by means of FESEM (Fig. 2a-e). The characterization was carried out to study the effect of activation and carbonization processes on surface morphology of the samples before and after impregnation, carbonization, and washing.

For the peat soil (Fig. 2a), the surface morphology was quite smooth and without any pores except for some occasional cracks or crevices. As it can be seen in the Fig. 2b, the $ZnCl_2$ structure (rod-like form) was obviously observed in the PS-ZIC sample. This finding agreed with the TGA results of the PS-ZI sample. $ZnCl_2$ was not successful in interacting with peat soil during the impregnation processes, due to the peat soil's properties, such as its low oxygen content. $ZnCl_2$ can be considered a Lewis acid, meaning it is able to interact with the non-bonding electrons of oxygen atoms in the precursor. The absence of non-bonding oxygen molecules in the precursor will reduce the ability of $ZnCl_2$ to interact with the peat soil. Therefore, molecules of $ZnCl_2$ (crystalized form) still remained in the PS-ZIC sample after the impregnation and carbonization.

The FESEM images of PS-PIC are given in Fig. 2c. This figure shows that the PS-PIC had a similar external surface morphology with the peat soil sample. No crystal structure of H_3PO_4 was observed in the PS-PIC sample. H_3PO_4 interacts with peat soil via acid hydrolysis processes. The H_3PO_4 will hydrolyze the glycosidic linkage in hemicellulose and cellulose and cleave the aryl bond in lignin (Jagtoyen and Derbyshire 1998) in low carbonization temperatures. This may allow a better interaction between the H_3PO_4 and peat soil.

As can be observed in Fig. 2d and Fig. 2e, it is obvious that the PSAC-Z-30 had fewer cavities than the PSAC-P-30. It seems that the cavities on the surfaces of PSAC-P-30 resulted from the evaporation of H_3PO_4 during carbonization, leaving behind the space previously occupied by the H_3PO_4. The removal of $ZnCl_2$ in the PSAC-Z-30 sample occurred after the second carbonization stage at 800 °C for 3 h without the presence of N_2. In this process, a high amount of $ZnCl_2$ was believed to be evaporated and then removed easily from the sample. Without the second carbonization, the $ZnCl_2$ residues still remained in the sample, even after it was refluxed with 0.2 M HNO_3 and washed with water. This may be due to the dissociation of $ZnCl_2$ into Zn^{2+} during the impregnation processes, thus reacting with complex molecules in peat soil to form stable polymorphs.

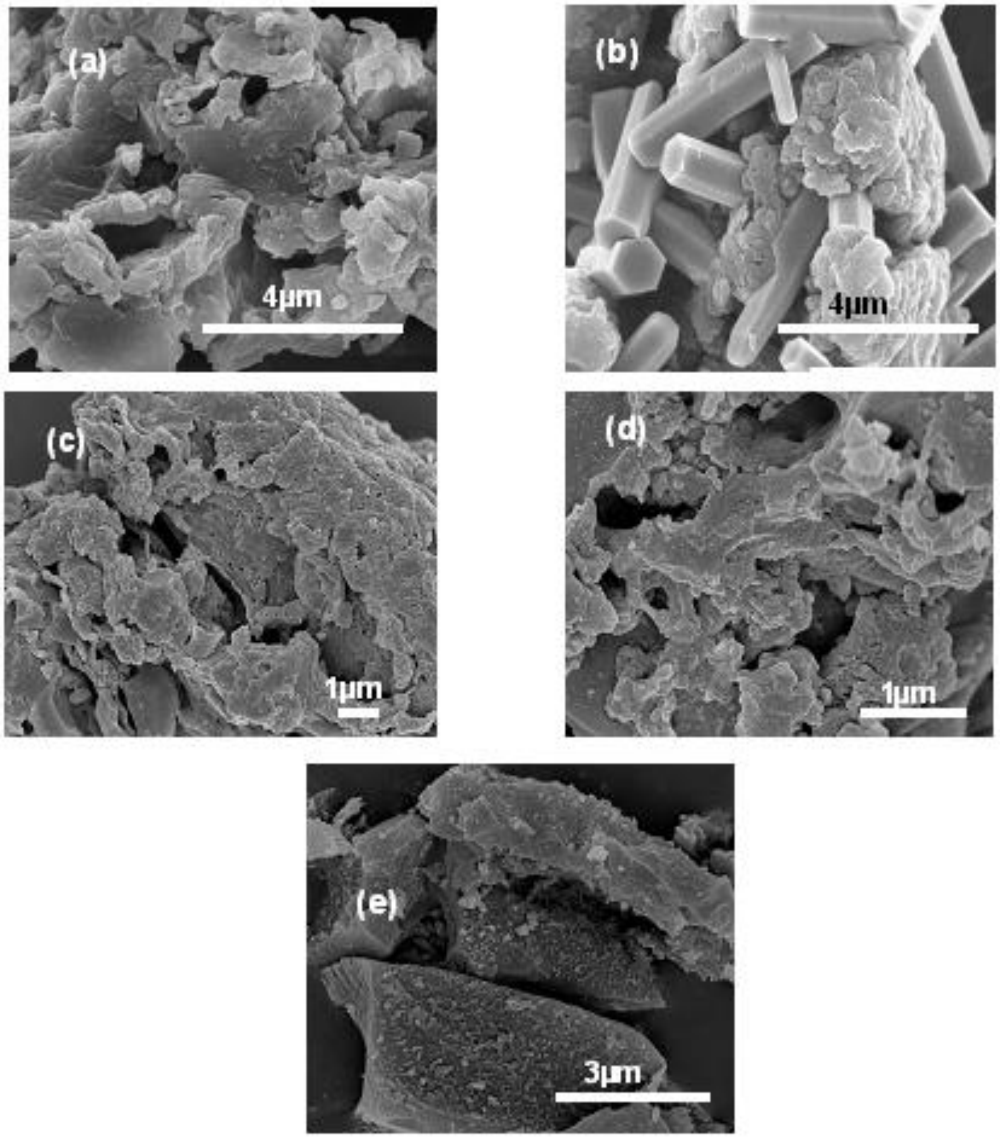

Fig. 2. FESEM images of (a) peat soil; (b) peat soil impregnated with 30% $ZnCl_2$, followed by carbonization at 500 °C for 3 h (PS-ZIC), (c) peat soil impregnated with 30% H_3PO_4, followed by carbonization at 500 °C for 3 h (PS-PIC), (d) peat soil activated carbon prepared using $ZnCl_2$ (30%) activation method (PSAC-Z-30), and (e) peat soil activated carbon prepared using H_3PO_4 (30%) activation method (PSAC-P-30)

Surface Area and Porosity Structure

The BET specific surface area, total pore volume, and average pore diameter of AC play an important role for it final application. These characteristics were used to determine the optimal condition for the preparation of AC. An overview of the main porous properties of the PSAC is provided by the results, as summarized in Table 3. Figures 3a-b illustrate the N_2 adsorption-desorption isotherms of PSAC prepared using different concentrations of H_3PO_4 and $ZnCl_2$, respectively. The BJH desorption pore size distribution of PSACs is shown in Fig. 4a-b.

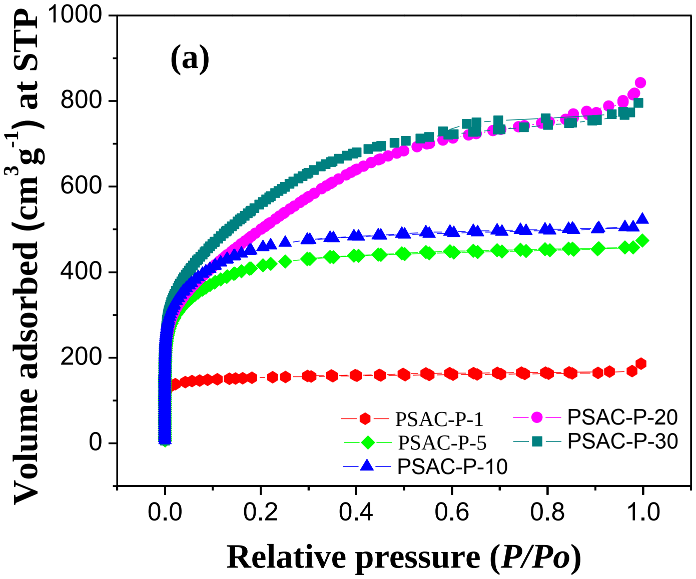

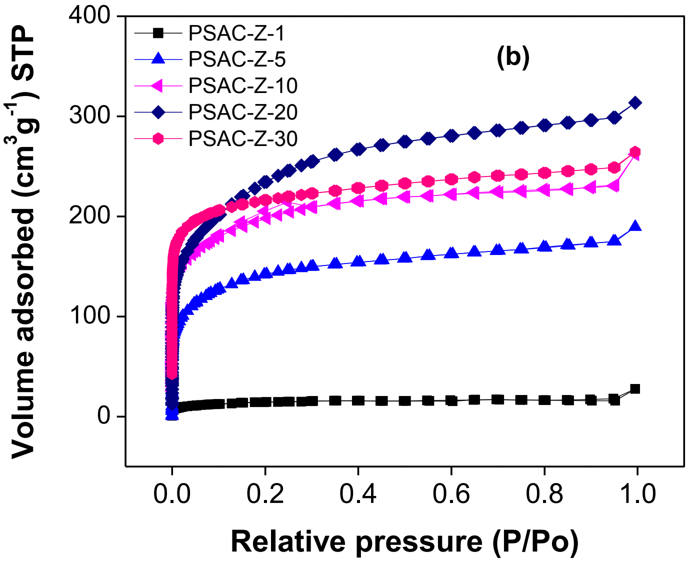

Fig. 3. N_2 adsorption-desorption isotherm of (a) peat soil activated carbon prepared using H_3PO_4 activation method (PSAC-P) and (b) peat soil activated carbon prepared using $ZnCl_2$ activation method (PSAC-Z) at different concentrations of H_3PO_4 and $ZnCl_2$. The samples were carbonized at 500 °C for 3 h.

As can be observed in Fig. 3a, the isotherms were predominantly Type I, according to the IUPAC classification (Sing *et al.* 1985). A type I isotherm refers to the adsorption of gases on microporous solids, for which the pore sizes are not much larger than the molecular diameter of the adsorbate. Complete filling of these narrow pores corresponds to the completion of a molecular monolayer of the adsorbate on the adsorbate surface. However, in the case of PSAC-P samples, which were prepared using 1, 5, and 10% H_3PO_4, a plateau was not clearly obtained, indicating a widening of pores. As a result, the isotherms actually exhibited a type H_4 hysteresis loop, which is a characteristic of slit-shaped pores. As the concentration of H_3PO_4 increased to 20% and 30%, the PSAC-P-20 and PSAC-P-30 exhibited a combination of Type I and Type II isotherms, indicated by the simultaneous presence of micro- and mesopores. A similar simultaneous micro- and mesopore property was also observed by Baquero *et al*. (2003) on their AC samples prepared from coffee bean husks, using H_3PO_4 chemical activation. The isotherms of PSAC-P-20 and PSAC-P-30 exhibited a well-defined plateau and knee, with open hysteresis loops, extending to a relative pressure of $P/P_o \approx 1.0$, indicating a mesopore-rich texture.

PSAC prepared using 1, 5, 10, 20, and 30% $ZnCl_2$ showed a Type I isotherm, as presented in Fig. 3b. The PSAC prepared using 10, 20, and 30% $ZnCl_2$ showed a well-defined plateau and knee, extending to a relative pressure of $P/P_o \approx 1.0$, indicating a mesopore-rich texture. The same was also observed in PSAC-P samples. Further increases of the activating agent concentration resulted in increases of N_2 uptake. Nevertheless, the N_2 uptake decreased, by increasing the $ZnCl_2$ concentration up to 30%. This may be due to the higher concentration of $ZnCl_2$, resulting in most of the peat soil surface structure being occupied by $ZnCl_2$. $ZnCl_2$ salts were not totally leaving the peat soil sample during reflux and washing, thus blocking some of the pore entrances to the N_2 molecules. This problem usually happens for the AC samples prepared with high activating agent concentrations (Ahmadpour and Do 1997).

Fig. 4a-b represents the pore size distribution of the PSAC-P and PSAC-Z prepared using different concentrations of H_3PO_4 and $ZnCl_2$, respectively. The pore size distribution represents a model of the internal structure of an AC sample (Ismadji and Bhatia 2001). As shown in Fig. 4a-b, this confirms that the PSAC-P and PSAC-Z produce mainly micropores and some mesopores at different concentrations of the activating agent. With the increase of the activating agent concentration, the creation of the micropore structure and the widening of micropore to mesopore occur simultaneously.

The effects of different activating agents (H_3PO_4 and $ZnCl_2$) and different activating agent concentrations on the BET specific surface area (S_{BET}), average pore diameter, and total pore volume (V_{pore}) are given in Table 3. The S_{BET} is the main indicator for the surface properties of AC, as described by Chandra *et al*. (2009) and Kalderis *et al*. (2008). As indicated in Table 3 and Fig 4(a), the S_{BET} and V_{pore} increased with an increase of H_3PO_4 concentration. A slightly different trend occurred when $ZnCl_2$ was used (PSAC-Z).

The increase in porosity with an increasing H_3PO_4 concentration can be attributed to the ability of H_3PO_4 hydrolyzed cellulose, lignocellulose, and lignin in the peat soil during the impregnation step. At this step, H_3PO_4 promotes the bond cleavage in the biopolymers structure (Jagtoyen and Derbyshire 1993). The increase in H_3PO_4 concentration will increase the bond cleavage processes.

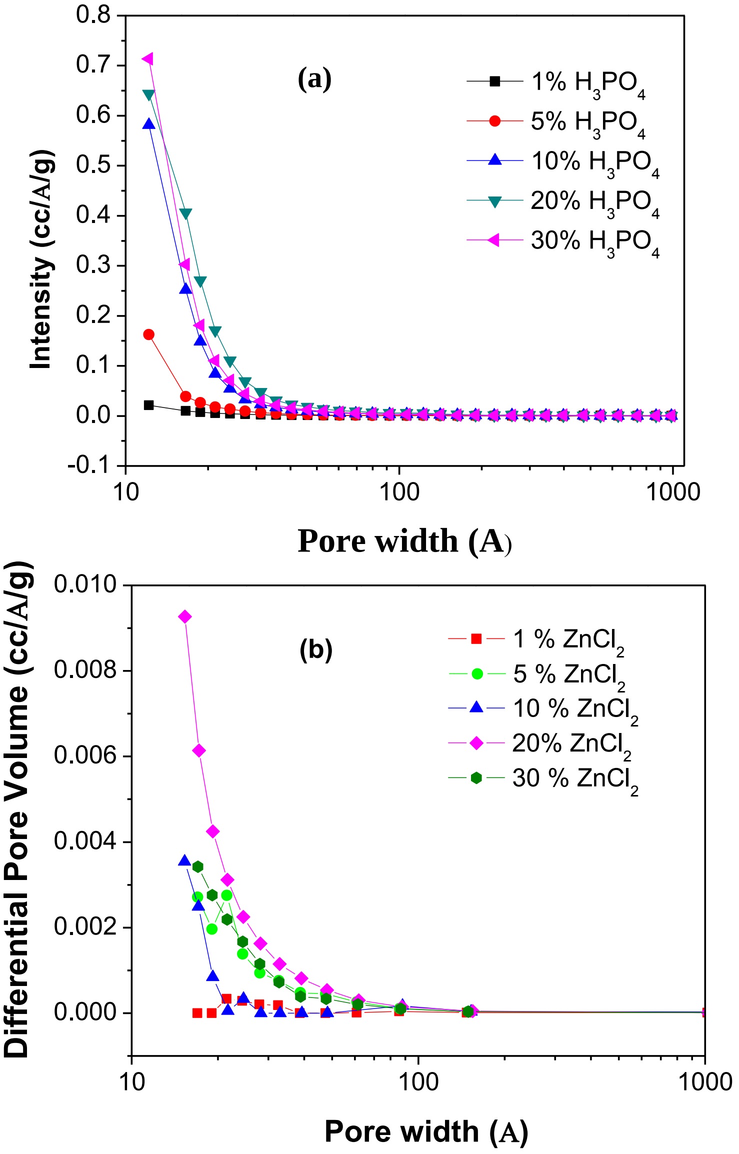

Fig. 4. Pore size distribution based on BJH desorption method of (a) PSAC-P and (b) PSAC-Z prepared using different H_3PO_4 and $ZnCl_2$ concentrations, respectively

During the carbonization processes, the weight loss rate of the precursor considerably slows because H_3PO_4 exhibits the formation of volatile cellulose products (Delgado and Mendez 2011); thus, the peat soil structure begins to dilate. This dilation is related to the cross-linking reactions between the biopolymer chains, *via* the formation of ester linkages between H_3PO_4 and OH groups in the precursor (Delgado and Mendez 2011). As the H_3PO_4 concentration increases, the weight loss rate slows, leading to an increase in the formation of aromatic rings and the dilation of precursor pore structure. Therefore, after the elimination of the phosphate group by the washing step, the obtained AC matrix remains dilated, leaving an accessible pore structure.

The increase in porosity with the $ZnCl_2$ concentration could be explained by the ability of $ZnCl_2$ to act as a Lewis acid to react with the OH groups in the precursor. During the impregnation step, the degradation of biopolymers structure is promoted by the high acidity of the $ZnCl_2$. The functional groups in the precursor can react with the $ZnCl_2$ by forming Zn-O complexes, followed by the elimination of water. After this reaction, the biopolymers are transformed into randomly oriented carbon structures that generate cavities (Delgado and Mendez 2011). However, the porosity properties of PSAC prepared using $ZnCl_2$ are lower than those of PSAC prepared using H_3PO_4 activation; this may be due to $ZnCl_2$ only being able to interact with the nonbonding electrons of oxygen atoms in the precursor. Nevertheless, peat soil has a complex chemical structure, and it contains less oxygen content. As a conclusion, the optimal condition for the preparation of PSAC with high BET surface area is using 30% H_3PO_4 as the activation agent.

Table 3. Characteristic of the Porous Structure of the PSAC-P and PSAC-Z

Sample	Conc. of activating agent (%)	Surface area (m^2/g)	Pore volume (cc/g)	Pore width (Å)
PSAC-P-1	1	373	0.28	30
PSAC-P-5	5	1081	0.72	27
PSAC-P-10	10	1491	1.15	29
PSAC-P-20	20	1596	1.29	32
PSAC-P-30	30	1974	1.41	32
PSAC-Z-1	1	47	0.02	15
PSAC-Z-5	5	461	0.07	18
PSAC-Z-10	10	673	0.08	18
PSAC-Z-20	20	794	0.11	18
PSAC-Z-30	30	640	0.19	16

The surface area result of PSAC obtained in this study was compared with PSAC obtained by previous works (Table 4). The results indicate that the AC prepared using peat soil as the precursor with 30% H_3PO_4 as the chemical activator has the largest surface area with the formation of micro- and mesopores structure.

Table 4. Effect of Activation Methods and the BET Specific Surface Area on the Yields of AC

Methods	Precursor	AC yields (%)	Surface area (m_2/g)	References
H_3PO_4 chemical activation	Tropical peat soil	50.1	1974	Our method
$ZnCl_2$ chemical activation	Tropical peat soil	48.9	794	Our method
Physical activation	Tropical peat soil	-	889	Ogawa *et al.* 2011
Physical activation	Tropical peat soil	-	900	Uraki *et al*. 2009
H_3PO_4 chemical activation	Durian shell	-	1404	Tham *et al*. 2011
H_3PO4 chemical activation	Cattail	-	1279	Shi *et al*. 2010
H_3PO_4 chemical activation	Maize tassel	-	1262	Olorundare *et al*. 2012
H_3PO_4 chemical activation	Grape seeds	-	1139	Bahri *et al.* 2012
$ZnCl_2$ chemical activation	Oil palm shells	-	1429	Allwar *et al*. 2008

These results clearly demonstrated that using H_3PO_4 chemical activation and peat soil as the carbon precursor could resulted in high adsorption capacity, which is important for various applications. This result also shows that the H_3PO_4 chemical activation method is an effective method in producing AC based-peat soil with high BET specific surface area.

Raman Spectroscopy

Further study was carried out by analyzing the PSAC-P and PSAC-Z samples, using Raman spectroscopy, to identify the graphitic nature of the ACs obtained. The great versatility of AC materials arises from the strong dependence of their physical properties. Generally, the physical properties of AC can be determined based on the ratio of sp^2 (graphite-like) to sp^3 (diamond-like) carbon, I_G/I_D (Ferrari and Robertson 1999). The Raman spectra of the PSAC-P and PSAC-Z samples are composed of two sharp peaks, known as the D (disordered) (~1350 cm^{-1}) and G (ordered or graphitic) (~1597 cm^{-1}) bands.

Figures 5a and 5b illustrate the Raman spectra of the PSAC-P and PSAC-Z samples, respectively. The G bands in the Raman spectra for both PSAC show that the PSAC samples contained sp^2 carbon networks (graphite-like). The sp^2 carbon network can exist in either C=C chains or aromatic ring structures (Rebollo-Plata *et al*. 2005). The D band in the Raman spectra refers to defects of the graphitic characteristic of the samples; it is also known as disordered graphite.

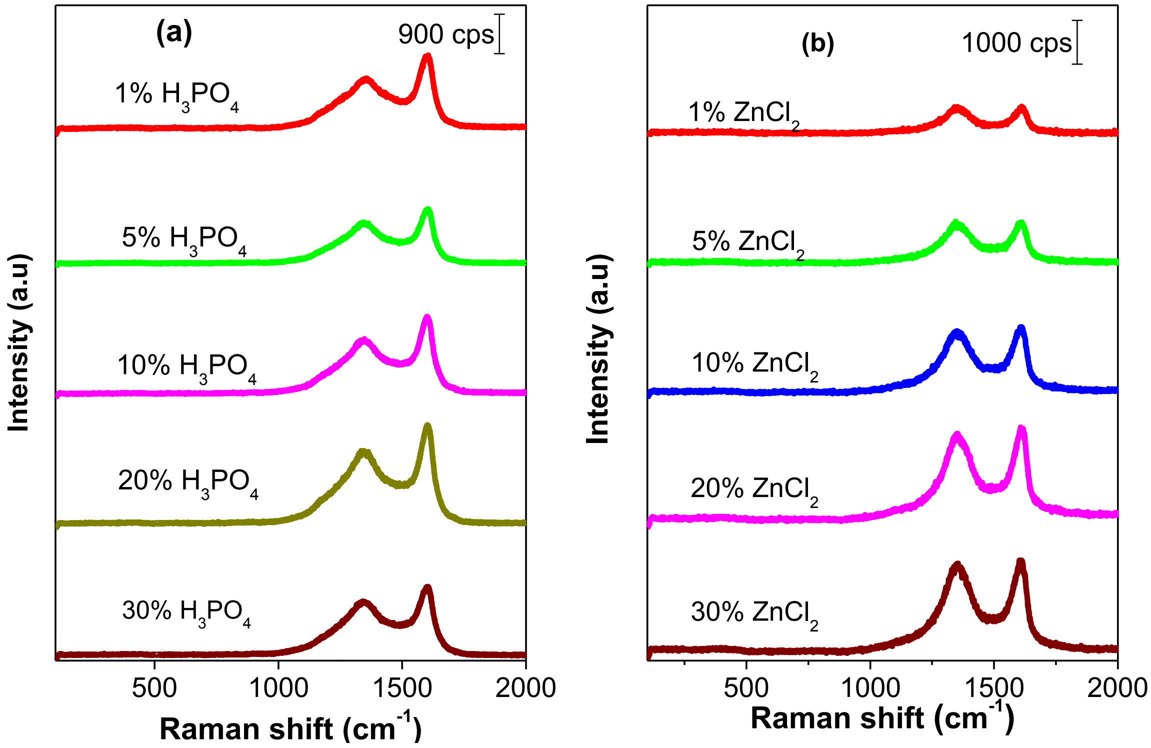

Fig. 5. Raman spectra of PSAC prepared using different concentrations of (a) H_3PO_4 and (b) $ZnCl_2$

Figure 6 shows a plot of the I_G/I_D value of the PSAC-P and PSAC-Z samples. Based on Fig. 6, it is revealed that the PSAC prepared using 5% H_3PO_4 achieved the highest I_G/I_D

value (1.4), while in the case of $ZnCl_2$ activation, 10% concentration reached the highest I_G/I_D value (0.95). This finding showed that an increase in the activation agent concentration will increase the graphitic nature of the PSAC samples. Nevertheless, further increases of the activation agent concentration will decrease the graphitic nature of PSAC. A higher activation agent concentration may increase the hydrolysis capabilities, thus increasing the degradation process on biopolymers. Therefore, it may cause the decrease of the graphitic nature of PSAC. However, the intensity of the Raman peaks increased, presumably due to the increase in the carbon yield (Fig. 5a-b).

Figure 6 also illustrates that the I_G/I_D value of PSAC prepared using H_3PO_4 was always higher than that of $ZnCl_2$, indicating that the PSAC-P had a more graphitic character (higher ordering of the graphitic structure) (Tuinstra and Koenig 1970; Angoni 1998), compared to PSAC-Z. This may be due to the properties of $ZnCl_2$ during activation processes. It is believed that the existence of a reasonable graphitic content in the sample improved the strength and thermal conductivity properties of the PSAC, thereby improving its suitability as a framework material for PCM as TES materials.

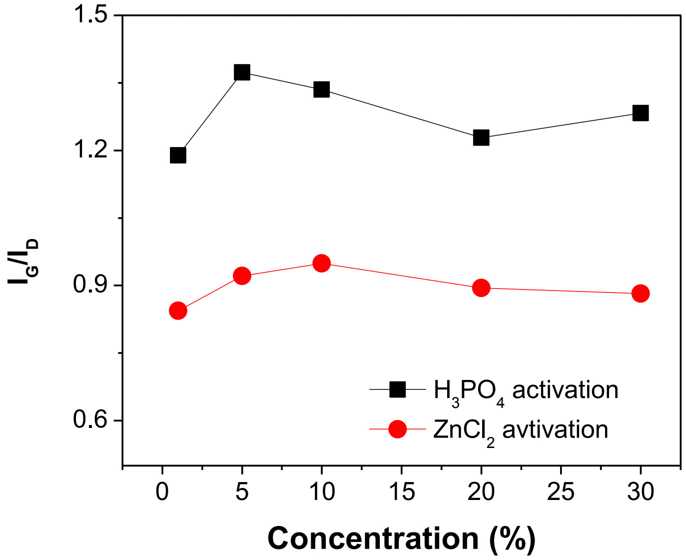

Fig. 6. Plot of I_D/I_G value of PSAC prepared using different concentrations of H_3PO_4 and $ZnCl_2$ activation methods

Surface Chemistry

The AC matrix does not consist of carbon atoms alone. It is also formed by various heteroatoms, such as hydrogen, oxygen, nitrogen, sulfur, phosphorus, and many more. These heteroatoms are bonded to the edges of the carbon layers, which control the surface chemistry of AC (Prahas *et al*. 2008). Basically, the surface of AC can be characterized by determining their acidity and basicity properties. The surface chemistry is an important characteristic that should properly be studied to make sure that the AC obtained fits their final application. For the TES, surface chemistry plays an important role to ensure that the PCM can totally be infiltrated into the pores of AC. PCM infiltrated into the pores of AC is preferred because the pores of AC can act as a capsule, stabilizing PCM and thus protecting PCM from a liquid leakage problem during its phase change processes. In this study, PSAC-P and PSAC-Z were characterized using FTIR to determine their surface chemistry.

FTIR spectra of PSAC-P and PSAC-Z prepared using various activation agent concentrations are illustrated in Fig. 7a-b. Figure 7a shows that the absorption band at around 3600 to 2400 cm^{-1} disappeared for the samples prepared using 1 to 30 % H_3PO_4. The band disappeared due to the formation of polyphosphate and inorganic species in the carbon (Hesas *et al*. 2011). This finding shows that the H_3PO_4 activation can remove excess water and convert the methyl group in the precursor to AC with rich-pore structure. These results agree with the N_2 adsorption-desorption results. A peak at around 1710 cm^{-1} shows the presence of a stretching vibration of C=O in ketones, aldehyde, lactone, and carboxyl. The carboxyl, lactone, phenol, *etc.* have been reported to constitute surface acidity. The broadband between 1300 and 1000 cm^{-1} may be ascribed to the stretching mode of hydrogen bonded P=O, O-C stretching vibrations in the P-O-C linkage, and P=OOH, while the shoulder at 1080 to 1070 cm^{-1} can be assigned to the ionized linkage of P^+-O^- in acid phosphate esters (Puziy *et al*. 2005).

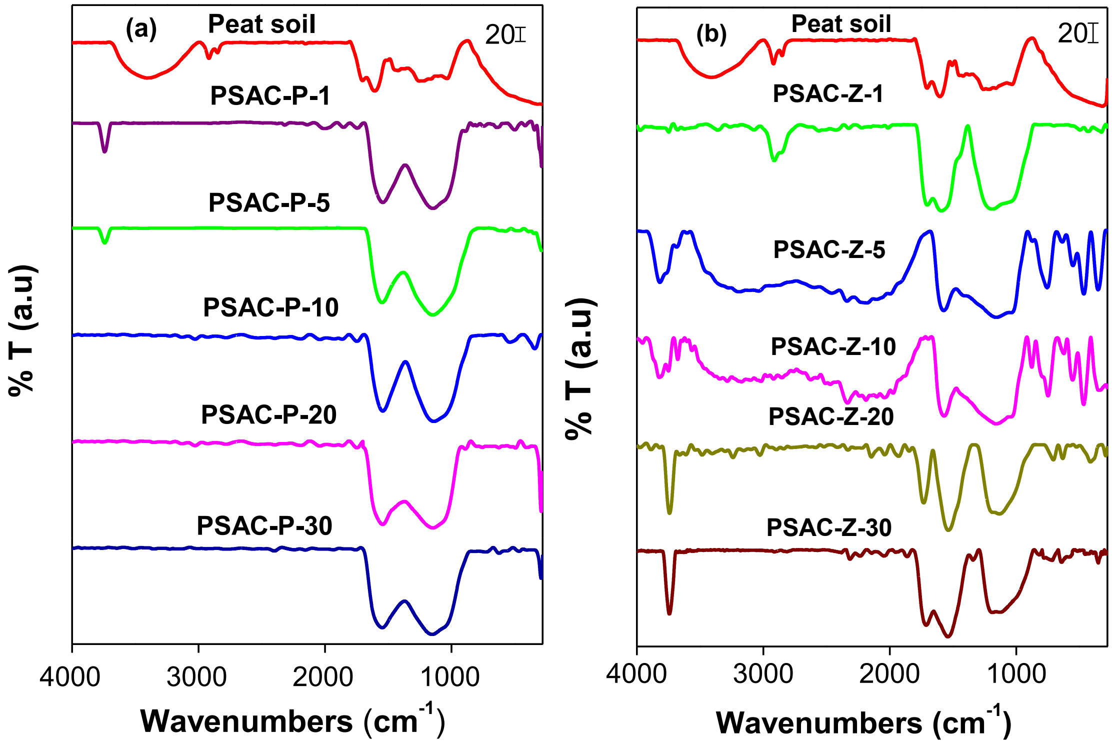

Fig. 7. FTIR spectra of PSAC prepared using different concentrations of (a) H_3PO_4 and (b) $ZnCl_2$

To summarize these findings, the FTIR spectra characterization (Fig. 7a-b), illustrated that PSAC-P and PSAC-Z gave similar functional groups, which shows that both samples have similar surface chemical reactivity. The small changes in the FTIR intensity were observed by increasing the concentration of both activating agents. It is shows that the activation processes start to occur even at low concentration of the activation agent as low as 1 wt.%

A different surface chemistry was observed in the PSAC-Z samples. Figure 7b shows that the increasing $ZnCl_2$ concentration increased the absorbance band intensity around 3800 cm^{-1}, which can be assigned to the hydroxyl group. The very weak peak at around 2900 cm^{-1}, observed in PSAC-Z-1, is a stretching vibration in the methyl group. This band was slowly eliminated by the increase of the $ZnCl_2$ concentration. A strong band at around 1710 cm^{-1} shows the presence of a stretching vibration of C=O ketones, aldehyde, lactones, and carbonyl. Another strong band at 1590 cm^{-1} can be attributed to the C=C aromatic ring stretching vibration (Puziy *et al*. 2005). The presence of a broad band between 1300 and 1000 cm^{-1} was also observed in the PSAC-Z samples.

XRD Patterns

XRD patterns of the peat soil and PSAC are displayed in Fig. 8. Based on the intensity evolution of the XRD patterns, the AC process can be viewed as consisting of two regions, a non-activated carbon region and an activated carbon region, corresponding to the untreated peat soil and chemical-activated peat soil using H_3PO_4 or $ZnCl_2$, respectively. The XRD patterns of the chemical-treated PSAC show a broad peak at $2\theta = 26^o$, which is attributable to the non-crystalline property of the PSAC. The XRD patterns show that there was no significant difference in terms of crystallinity of PSAC produced using different activation agents. As observed in Fig. 8a and Fig. 8b, the intensity of PSAC-P was higher than that of PSAC-Z, which indicates a higher crystal structure in the former. This finding agreed nicely with the Raman spectroscopy results.

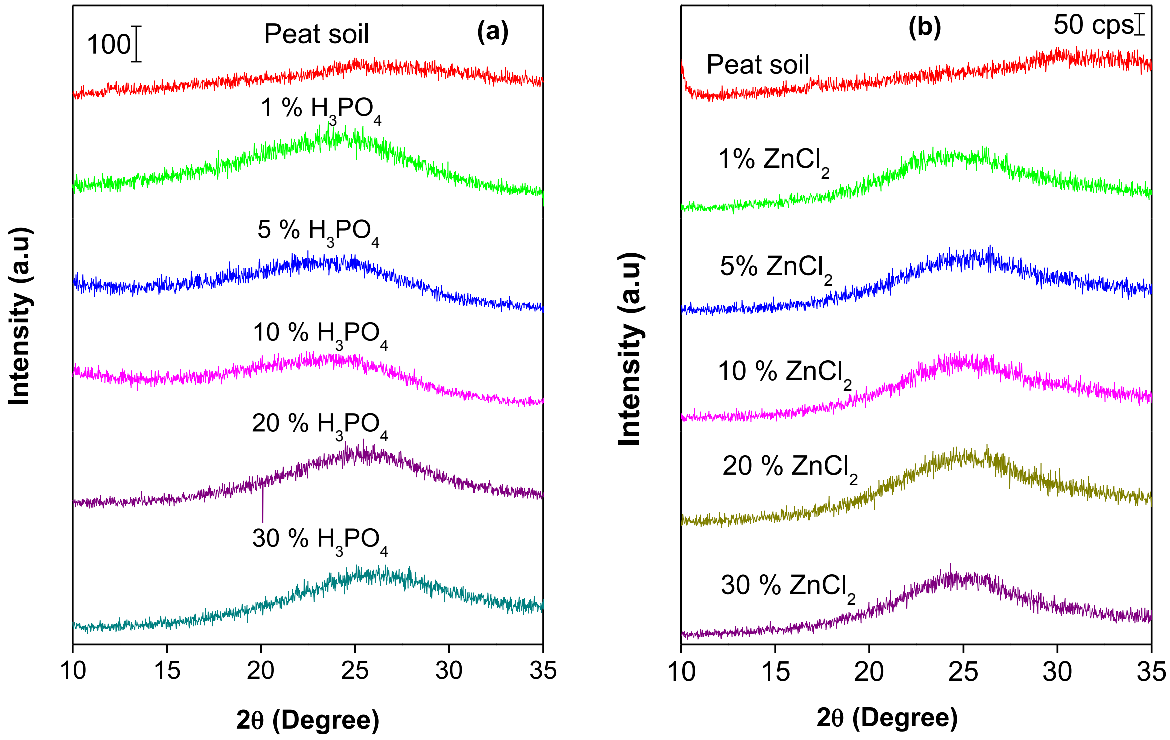

Fig. 8. XRD patterns of PSAC prepared using 1, 5, 10, 20, and 30% of (a) H_3PO_4 and (b) $ZnCl_2$

CONCLUSIONS

1. The results of this study showed that peat soil can be converted into activated carbon, using phosphoric acid (H_3PO_4) and zinc chloride ($ZnCl_2$) activation methods under N_2 gas atmosphere.

2. The pore structure and surface chemistry of the peat soil activated carbons can be tailored using different types and concentrations of activating agents. Peat soil activated carbon with well-developed pores (BET surface area = 1974 m^2/g, pore volume = 1.41 m^2/g, average pore width = 32 Å) is produced using 30% H_3PO_4 at carbonization temperature of 500 ^oC for 3 h.
3. H_3PO_4 facilitated the conservation of porous structures in the peat soil precursor and also lead to the creation of tremendous porosity, and resulted in various functional structures on the surface and in the bulk phases of the peat soil activated carbon.
4. The produced peat soil activated carbon is composed of graphitic carbon nanostructures formed by carbonization-oxidation-activation processes. However, peat soil activated carbon prepared using H_3PO_4 chemical activation processes has more graphitic character compared to PSAC prepared using $ZnCl_2$ chemical activation method.
5. The peat soil activated carbon revealed an improved adsorption performance with high crystallinity properties and therefore, it is suitable to be used in varies applications.

ACKNOWLEDGMENTS

This work was supported by the Ministry of Higher Education of Malaysia (MOHE), under grant no. FRGS/1/11/SG/UPM/01/2, and the JPA scholarship for Doctoral Program for TK is gratefully acknowledged.

REFERENCES CITED

Ahmadpour, A., and Do, D. D. (1997). "The preparation of activated carbon from macadamia nutshell by chemical activation," *Carbon* 35(12), 1723-1732. DOI: DOI: 10.1016/S0008-6223(97)00127-9

Allwar, Ahmad, M. N., and Mohd Asri, M. N. (2008). "Textural characteristics of activated carbons prepared from oil palm shells activated with $ZnCl_2$ and pyrolysis under nitrogen and carbon dioxide," *Journal of Physical Science* 19(2), 93-104.

Angoni, K. (1998). "A study of highly ordered carbons by used of macroscopic and microscopic Raman spectroscopy," *Journal of Material Sciences* 33(4), 3693-3698. DOI: 10.1023/A:1004628017725

Ariyadejwanich, P., Tanthapanichakoon, W., Nakagawa, K., Mukai, S. R., and Tamon, H. (2003). "Preparation and characterization of mesoporous activated carbon from waste tires," *Carbon* 41, 157-164. DOI: 10.1016/S0008-6223(02)00267-1

ASTM D 1997-91. (1996). "Standard test method for laboratory determination on the fiber content of peat samples by dry mass," *Annual Book of ASTM Standards,* ASTM. Philadelphia, USA.

ASTM D4318-05. (2005). "Test method for liquid limit, plastic limit and plasticity index of soils, ASTM International, USA.

Bahri, M. A., Calvo, L., Gilarranz, M. A., and Rodriguez, J. J. (2012), "Activated carbon from grape seeds upon chemical activation with phosphoric acid: Application to the adsorption of diuron from water," *Chemical Engineering Journal* 203, 348-356. DOI: 10.1016/j.cej.2012.07.053

Baquero, M. C., Giraldo, L., Moreno, J.C., Suárez-García, F., Martínez-Alonso, A., and Tascón, J. M. D. (2003). “Activated carbons by pyrolysis of coffee bean husks in presence of phosphoric acid,” *Analytical Applied Pyrolysis* 70(2), 779-784 (ISSN 0165-2370). DOI: 10.1016/S0165-2370(02)00180-8

BS 1377 Part 1-4. (1990). “Soils for civil engineering purpose,” *British Standard Institution*, London, UK.

Cagnon, B., Py, X., Guillot, A., Stoeckli, F., and Chambat, G. (2009). “Contributions of hemicellulose, cellulose and lignin to the mass and the porous properties of chars and steam activated carbons from various lignocellulosic precursors,” *Bioresource Technol*ogy, 100, 292-298. DOI: 10.1016/j.biortech.2008.06.009

Caturla, F., Molina-Sabio, M., and Rodriguez-Reinoso, R. (1991). “Preparation of activated carbon by chemical activation with $ZnCl_2$,” *Carbon* 29(7), 999-1007. DOI: 10.1016/0008-6223(91)90179-M

Chandra, T. C., Mirna, M. M., Sunarso, J., Sudaryanto, Y., and Ismadji, S. (2009). “Activated carbon from durian shell: Preparation and characterization,” *Journal of the Taiwan Institute of Chemical Engineers* 40, 457-462. DOI: 10.1016/j.jtice.2008.10.002

Chen, Z., Shan, F., Cao, L., and Fang, G. (2012). “Synthesis and thermal properties of shape-stabilized lauric acid/activated carbon composites as phase change materials for thermal energy storage,” *Solar Energy Materials and Solar Cells* 102, 131-136. DOI: 10.1016/j.solmat.2012.03.013

Cheong, S.P., and Ng, S. K. (1977). “Major nutrient requirements of oil palm on deep acid peat in Malaysia,” Conference on Classification and Management of Tropical Soils, Kuala Lumpur, Malaysia.

Delgado, C. N., and Mendez, R. R. (2011). “Preparation of carbon materials from lignocellulosic biomass,” in: *Green Carbon Materials: Advances and Applications*, Rufford, T. E., Hulicova-Jurcakova, D., and Zhu, J. (eds.), Taylor and Francis Group, US, pp.35-57. DOI: 10.1201/b15651-3

Den Haan, E. J. (1997). “An overview of the mechanical behavior of peats and organic soils and some appropriate construction techniques,” in: *Proc. of the Conf. on Recent Advances in Soft Soil Engineering*, Kunching, Malaysia, Huat and Bahia (eds.), 1, 17-45.

Feng, L., Zheng, J., Yang, H., Guo, Y., Li, W., and Li, X. (2011). “Preparation and characterization of polyethylene glycol/active carbon composites as shape-stabilized phase change materials,” *Solar Energy Materials and Solar Cells* 95, 644-650. DOI: 10.1016/j.solmat.2010.09.033

Fernández, F., Valenciano, J., Trinidad, F., and Munóz, N. (2010). “The used of activated carbon and graphite for the development of lead-acid batteries for hybrid vehicle applications,” *Journal of Power Sources* 195, 4458-4469. DOI: 10.1016/j.jpowsour.2009.12.131

Ferrari, A. C., and Robertson, J. (1999). “Interpretation of Raman spectra of disordered and amorphous carbon,” *Physical Review B* 61(20), 14094-107. DOI: http://dx.doi.org/10.1103/PhysRevB.61.14095

Frackowiak, E., and Béguin, F. (2001). “Carbon materials for the electrochemical storage of energy in capacitors,” *Carbon* 39, 937-950. DOI: 10.1016/S0008-6223(00)00183-4

Fierro, V., Muñiz, G., Basta, A. H., El-Saied, H., and Celzard, A. (2010). “Rice straw as precursor of activated carbons: Activation with ortho-phosphoric acid,” *Journal of Hazardous Materials* 181, 27-34.DOI: 10.1016/j.jhazmat.2010.04.062

González-Garía, P., Centeno, T.A., Urones-Garrote, E., Āvila-Brande, D., and Otero-Díaz, S. (2013). "Microstructure and surface properties of lignocellulosic-based activated carbons," *Applied Surface Science* 265, 731-737. DOI: 10.1016/j.apsusc.2012.11.092

Hesas, R. H., Wan Daud, W. M. A., Sahu, J. N., and Arami-Niya, A. (2011). "The effects of a microwave heating method on the production of activated carbon from agricultural waste," *Journal of Analytical and Applied Pyrolysis* 100, 1-11. DOI: 10.1016/j.jaap.2012.12.019

Hussein, M. Z., Tarmizi, R. S. H., Zainal, Z., and Ibrahim, R. (1996). "Preparation and characterization of active carbons from oil palm shells," *Carbon* 34(11), 1447-1454. DOI: 10.1016/S0008-6223(01)00147-6

Ibarra, J. V., Moliner, R., and Palacios, J. M. (1991). "Catalytic effects of zinc chloride in the pyrolysis of Spanish high sulfur coals," *Fuel* 70, 727-732. DOI: 10.1016/0016-2361(91)90069-M

Ioannidou, O., and Zabaniotou, A. (2007). "Agricultural residues as precursors for activated carbon production – A review," *Renewable and Sustainable Energy Reviews*, 11:1966-2005. DOI:10.1016/j.rser.2006.03.013

Islam, M. D., and Hashim, H. (2010). "Behaviour of stabilized peat: A field study," *Scientific Research and Essay* 5(17), 2366-2374.

Ismadji, S., and Bhatia, S. K. (2001). "Characterization of activated-carbons using liquid phase adsorption," *Carbon* 39, 1237-1250. DOI: 10.1016/S0008-6223(00)00252-9

Jagtoyen, M., and Derbyshire, F. (1993). "Some considerations of the origins of porosity in carbons from chemically activated wood," *Carbon* 31(7), 1185-1192. DOI: 10.1016/0008-6223(93)90078-O

Jagtoyen, M., and Derbyshire, F. (1998). "Activated carbons from yellow poplar and white oak by H_3PO_4 activation," *Carbon* 36(7-8), 1085-1097. DOI: 10.1016/S0008-6223(98)00082-7

Kalderis, D., Bethanis, S., Paraskeva, P., and Daimadopulos, E. (2008). "Production of activated carbon from bagasse and rice husk by single-stage chemical activation method at low retention times," *Bioresources Technology* 99, 6809-6816. DOI: 10.1016/j.biortech.2008.01.041

Khalili, N. R., Campbell, M., Sandi, G., and Golaś, M. (2000). "Production of micro and mesoporous activated carbon from paper mill sludge: 1. Effect of zinc chloride activation," *Carbon* 38, 1905-1915. DOI: 10.1016/S0008-6223(00)00043-9

Kong, J., Yue, O., Huang, L., Gao, Y., Sun, Y., Gao, B., Li, O., and Wang, Y. (2013). "Preparation, characterization and evaluation of adsorptive properties of lather waste based activated carbon via physical and chemical activation," *Chemical Engineering Journal* 221, 62-71. DOI: 10.1016/j.cej.2013.02.021

Liu, Y., Guo, Y., Gao, W., Wang, Z., Ma, Y., and Wang, Z. (2012). "Simultaneous preparation of silica and activated carbon from rice husk ash," *Journal of Cleaner Production* 32, 204-209. DOI: 10.1016/j.jclepro.2012.03.021

Lucas, R. E. (1982). "Organic salts (Histosol). Formation, distribution, physical and chemical properties and management for crop production," Michigan State University, Research Report No. 435 (Farm Science).

Mochida, M., Fotoohi, B., Amamo, Y., and Mercier, L. (2012). "Cadmium (II) and lead (II) adsorption onto hetero-atom functional mesoporous silica and activated carbon," *Applied Surface Science* 258, 7389-7394. DOI: 10.1016/j.apsusc.2012.04.042

Molino-Sabio, M., Rodriguez-Reinoso, F., Caturla, F., and Sellés, M. J. (1995). "Porosity in granular carbons activated with phosphoric acid," *Carbon* 33(8), 1105-1117.DOI: 10.1016/0008-6223(95)00059-M

Mozammel, H. M., Masahiro, O., and Bhattacharya, S. C. (2002). "Activated charcoal from coconut shell using $ZnCl_2$ activation," *Biomass Energy* 22, 397-400.DOI: 10.1016/S0961-9534(02)00015-6

Mutalib, A. A., Lim, J. S., Wong, M. H. and Koonvai, L. (1992). "Characterization, distribution and utilization of peat in Malaysia," in: Aminuddin, B. Y. (ed.), Proceedings of the International Symposium on Tropical Peatland, Kuching, Serawak, Malaysia. MARDI, Kuala Lumpur, pp.7-16.

Nohara, L. B., Filho, G. P., Nohara, E. L., Kleinke, M. U., and Rezende, M. C. (2005). "Evaluation of carbon fiber surface treated by chemical and cold plasma processes," *Material Research* 8(3), 281-286. http://dx.doi.org/10.1590/S1516-14392005000300010

Ogawa, M., Bardant, T. B., Sasaki, Y., Tamai, Y., Tokura, S., and Uraki, Y. (2011). "Electricity-free production of activated carbon from biomass in Borneo to improve water quality," *BioResources* 7(1), 236-245.

Olorundare, O. F., Krause, R. W. M., Okonkwo, J. O., and Mamba, B. B. (2012). "Potential application of activated carbon from maize tessel for the removal of heavy metals in water," *Physics and Chemistry of the Earth* 50-52, 104-110. DOI: 10.1016/j.pce.2012.06.001

Otawa, T., Nojima, Y., and Miyazaki, T. (1997). "Development of KOH activated high surface area carbon and its application to drinking water purification," *Carbon* 35(9), 1315-1319. DOI: 10.1016/S0008-6223(97)00076-6

Rebollo-Plata, B., Lozada-Morales, R., Palomino-Merino, P., Davila-PintLe, J.A., Portillo-Mareno, O., Zelaya-Angel, O., and Jiménez-Sandoval, S. (2005). "Amorphous carbon thin films prepared by electron-gun evaporation," *The AZo Journal of Materials Online* 1-6. (DOI: 10.2240/azojomo0157).

Petrova, B., Budinova, T., Tsyntsarski, B., Kochcodan, V., Shkavro, Z., and Petrov, N. (2010). "Removal of aromatic hydrocarbons from water by activated carbon from apricot stones," *Chemical Engineering Journal* 165, 258-264. DOI: 10.1016/j.cej.2010.09.026

Prahas, D., Kartika, Y., Indraswati, N., and Ismadji, S. (2008). "Activated carbon from jackfruit peel waste by H_3PO_4 chemical activation: Pore structure and surface chemistry characterization," *Chemical Engineering Journal* 140, 32-42. DOI: 10.1016/j.cej.2007.08.032

Puziy, A. M., Poddubnaya, O. I., Martínez-Alonso, A., Suárez-García, F., and Tascón, J. M. D. (2005). "Surface chemistry of phosphorus-containing carbons of lignocellulosic origin," *Carbon* 43(14), 2857-2868. DOI: 10.1016/S0008-6223(05)00505-1

Sekar, M., Sakthi, V., and Rengaraj, S. (2004). "Kinetics and equilibrium adsorption study of lead (II) onto activated carbon prepared from coconut shell," *Journal Colloid Interface Science* 279, 307-313. DOI: 10.1016/j.jcis.2004.06.042

Selvakumar, M., and Bhat, D. K. (2012). "Microwave synthesized nanostructured TiO_2 activated carbon composite electrodes for supercapacitor," *Applied Surface Science*. DOI: org/10.1016/j.apsus. 2012.09.036.

Shi, Q., Zhang, J., Zhang, C., Li, C., Zhang, B., Hu, W., and Zhao, R. (2010). "Preparation of activated carbon from cattail and its application for dyes removal," *Journal of Environmental Sciences* 22(1), 91-97. DOI:10.1016/S1001-0742(09)60079-6.

Sing, K. S. W., Everett, D. H., and Haul, R. A. W. (1985). "Reporting physisorption data for gas/solid systems with special reference to the determination of surface area and porosity," *Pure Applied Chemistry* 57, 603-19. DOI: 10.1002/9783527610044.hetcat0065

Skubiszewska-Zieba, J. (2010). "VPO catalysts synthesized on substrates with modified activated carbons," *Applied Surface Science* 256, 5520-5527. DOI: 10.1016/j.apsusc.2009.12.129

Srinivasakannan, C. and Bakar, M. Z. A. (2004). "Production of activated carbon from rubber wood sawdust," *Biomass Bioenergy* 27, 89-96. DOI: 10.1016/j.biombioe.2003.11.002

Stavropoulo, G. G., and Zabaniotou, A. A. (2005). "Production and characterization of activated carbons from olive-seed waste residue," *Microporous Mesoporous Material* 83, 79-85. DOI: 10.1016/j.micromeso.2005.03.009

TAPPI. (1999). "Alpha-, beta- and gamma-cellulose in pulp," T203 om 93, Technical Association of the Pulp and Paper Industry, Atlanta, USA.

TAPPI. (2002). "Acid-insoluble lignin in wood and pulp," T222 om 02, Technical Association of the Pulp and Paper Industry, Atlanta, USA.

Tham, Y. J., Puziah, A. L., Abdullah, A. M., Shamala-Devi, A., and Taufiq-Yap, Y. H. (2011). "Performance of toluene removal by activated carbon derived from durian shell," *Bioresource Technology* 102, 724-728. DOI: 10.1016/j.biortech.2010.08.068

Tongpoothorn, W., Sriuttha, M., Homchan, P., Chanthai, S., and Ruangviriyachai, C. (2011). "Preparation of activated carbon derived from *Jatropha curcas* fruit shell by simple thermo-chemical activation and characterization of their physico-chemical properties," *Chemical Engineering Research and Design* 89, 335-340. DOI:10.1016/j.cherd.2010.06.012.

Torregrosa-Macia, R., Martin-Martinez, J. M., and Mittelmeijer-Hazeleger, M. C. (1997). "Porous texture of activated carbons modified with carbohydrates," *Carbon* 35(4), 447-453. DOI: 10.1016/S0008-6223(97)83724-4

Tuinstra, F., and Koenig, J. L. (1970). "Raman spectrum of graphitic," *The Journal of Chemical Physics* 53(3), 1126-1130. http://dx.doi.org/10.1063/1.1674108

Uraki, Y., Tamai, Y., Ogawa, M., Gaman, S., and Tokura, S. (2009). "Preparation of activated carbon from peat," *BioResources* 4(1), 205-213.

Wang, C., Feng, L., Li, W., Zheng, J., Tian, W., and Li, X. (2012). "Shape-stabilized phase change materials based on polyethylene glycol/porous carbon composite: the influence of the pore structure of the carbon materials," *Solar Energy Material and Solar Cells* 105, 21-26. DOI: 10.1016/j.solmat.2012.05.031

Wise, L. E., Murphy, M., and D'Addieco, A. A. (1946). "Chlorite holocellulose, its fractionation and bearing on summative wood analysis and on studies on the hemicellulose," *Paper Trade J.* 122, 35-43.

Wong, M. H. (1991). "The distribution, characteristics and agricultural utilization of peat in Serawak," Kuching, Malaysia: Department of Agriculture in Serawak.

Wust, R. A. J, Marc Bustin, R., and Lavkulich, M. L. (2003). "New classification systems for tropical organic-rich deposits based on studies of the Tasek Bera Basin, Malaysia," *Catena* 53, 133-163. DOI:10.1016/S0341-8162(03)00022-5

Yang, T., and Lua, A.C. (2006). "Textural and chemical properties of zinc chloride activated carbons prepared form pistachio-nut shells," *Material Chemistry and Physics* 100(2-3) 438-444.DOI: 10.1016/S0254-0584(06)00257-4

Article submitted: October 9, 2014; Peer review completed: November 19, 2014; Revised version received and accepted: December 3, 2014; Published: December 16, 2014.